Infrared Photometric Distance to WZ Hya

Camdon Ritterby (ORCID 0000-0002-6321-6461)
Department of Physics and Astronomy, Washington State University, Pullman, WA 99164-2814; camdon.ritterby@wsu.edu

Michael L. Allen (ORCID 0000-0002-6047-3315)
Department of Physics and Astronomy, Washington State University, Pullman, WA 99164-2814; mlfa@wsu.edu (corresponding author)

Received August 24, 2022; revised March 29, 2023; accepted April 5, 2023

Abstract A distance to the RR Lyrae star WZ Hya was determined to test how well period-luminosity-metallicity (PLZ) relations agree with current parallax measurements from Gaia. We obtained 120 photometric observations in the B, V, ip, and zs filters from 16 February to 28 May 2022. Fluxes were extracted using six-aperture photometry methods. The period found for WZ Hya was 0.5377 ± 0.0005 day. Using the theoretical PLZ relations, a weighted average distance of 872 ± 47 parsecs was determined for the V, ip, and zs filters with a minimization technique. This distance is compared to the distances found using color excess values found in the literature, which distances were 942 ± 51 and 931 ± 50 parsecs, respectively. The Gaia Data Release 3 (DR3) parallax distance is 999 ± 16 parsecs. The distances determined using the PLZ relation are consistent with the parallax-determined value from Gaia within 1–2 standard deviations.

1. Introduction

RR Lyrae stars are variable stars that belong to the horizontal branch. Their periods range from 0.2 to 1.2 days (Dambis et al. 2013). These pulsating stars are used as standard candles that help us understand the structure of the Milky Way. RR Lyr standard candles use period-luminosity relations to measure distances, then Catelan *et al.* (2004) and Cáceres and Catelan (2008) derived theoretical period-luminosity-metallicity relations that use the infrared ip and zs filters and the visible Johnson V filter. The standard for geometric parallax distances is the Gaia survey (Gaia Collaboration 2022). The infrared PLZ relations have not yet been determined to agree with those values found in Gaia for many stars. This research provides the results of these relations using the RR Lyr star WZ Hya and compares them to the parallax measurements determined by the Gaia DR3 survey.

WZ Hya is classified as an RRab type variable sstar (Clube *et al.* 1969). RRab-type variable stars can be determined by looking at the shape of their light curves. Known as fundamental-mode pulsating RR Lyr stars, these variable stars have an asymmetric light curve that has a steep rise and a much slower decline in magnitude. This typically takes the shape of a shark tooth. These light curves are provided in Figure 2 and basic properties of WZ Hya are found in Table 1.

This paper will first discuss how observations for WZ Hya were set up using the Las Cumbres Observatory (LCO) via Michael Fitzgerald's OurSolarSiblings (OSS) research course. The data pipelines set up to analyze these observations are discussed, along with descriptions of the equipment used (section 2). Then, the results of the PLZ relation will be analyzed, specifically the period and the distance from Earth (section 3). Finally, a comparison is drawn to the distance produced by the Gaia DR3 survey using parallax (section 4).

We transformed Gaia's values for parallax, p (arcseconds), and parallax error Δp, to distance, d (parsecs), and distance error, Δd, using standard formulae:

$$d = \frac{1}{p}, \quad |\Delta d| = \frac{1}{p^2}\Delta p. \qquad (1)$$

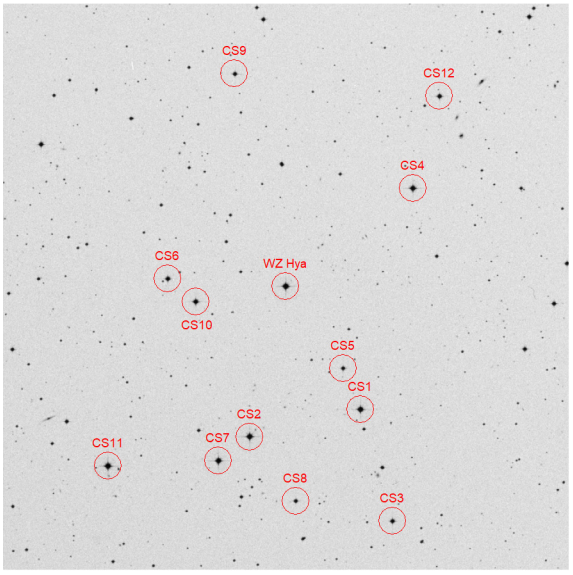

Figure 1. Field of WZ Hya with the 12 comparison stars used in data analysis. The image is 25 × 25 arcminutes. The image is from the Digitized Sky Survey (DSS) and is processed using SAOImageDS9. North is up and east is left.

2. Observations

WZ Hya was observed between February 16 and May 28, 2022. Figure 1 shows the field of WZ Hya and identifies the variable and comparison stars used. The star was observed through four filters: Johnson-Cousins B and V (Bessell 1993), SDSS ip (Sloan Digital Sky Survey; Fukugita *et al.* (1996)), and Pan-STARRS zs (Panoramic Survey Telescope and Rapid Response System; Tonry *et al.* (2012)). The star was observed with the Las Cumbres Observatory (LCO) network of robotic telescopes. The filter characteristics are summarized in Table 2.

Table 1. Basic properties of WZ Hya.

Property	*Value*	*Reference*	*Comments*
R.A. (J2000)	153.435053291387°	Gaia Collab. (2022)	Gaia DR3
Dec. (J2000)	–13.13816584777°	Gaia Collab. (2022)	
Spectral Type	A2	Barbier-Brossat *et al.* (1994)	
Variable Type	RRab	Clube *et al.* (1969)	
Parallax	1.0008 ± 0.0157 mas	Gaia Collab. (2022)	
Distance	999 ± 16 pc		From parallax; see text
Distance	982 ± 15 pc	Gaia Collab. (2022)	Photometric

Table 3 lists the location, telescope camera label, and the number of observations taken from all used telescopes. The WZ Hya dataset is shown in Appendix A and is also available through the AAVSO's public ftp site as noted in the Appendix.

Every observation of WZ Hya was taken using the 0.4-meter series of telescopes. Each was equipped with an SBIG STL-6303 CCD camera of format 3k × 2k pixels, with a pixel size of 0.571 arcsec and a field of view of 29.2 × 19.5 arcmins. Using the LCO observation portal, cadences were set up to provide an observation every four hours. In total, 120 observations of WZ Hya were recovered. All images produced by the LCO telescope network were usable.

Data gathered by the LCO telescope network needed to be optimized to allow data collection to still proceed without over-exposure occurring, avoiding errors in the photometric measurements being made. We used AstroImageJ ssoftware (Collins *et al.* 2017) on test images to measure approximate photon counts. Exposure times for our science run were calculated to collect 150,000 photons integrated. An exposure time was produced for each filter: 50 seconds for B, 20 seconds for ip, 18 seconds for V, and 80 seconds for zs.

The LCO's BANZAI data pipeline (Brown *et al.* 2013) took raw images from the telescope and corrected them using bad-pixel masking, bias subtraction, dark subtraction, flat field correction, and astrometric calibration. Source extraction and photometry were performed by the OurSolarSiblings (OSS) data pipeline (Fitzgerald 2018) automatically. The OSS pipeline trims and cleans up the images and then calculates a new World Coordinate System (WCS) value and applies it to the image. After this, six automated photometry methods are performed on each of the images, those being Dominion Astrophysical Observatory Photometry (DAO; Stetson 1987), DoPHOT (DOP; Schechter *et al.* 1993); Alonso-García *et al.* 2012), Source Extractor Aperture (SEX) and Source Extractor Kron (SEK) (Bertin and Arnouts 1996), Point Spread Function Extractor (PSX; Bertin 2011), and Aperture Photometry Tool (APT; Laher *et al.* 2012a, 2012b). For each star-like source, the results of these methods are then parsed into comma-separated variable files consisting of R.A., Dec., X and Y pixel values, counts, and errors in the counts.

Next, Astrosource software (Fitzgerald *et al.* 2020) was used to further process the data. Astrosource first identifies stars of sufficient signal-to-noise in the image. Then the least variable stars are chosen to become comparison stars. Next, the magnitudes of these calibration stars are extracted from photometric databases. Photometric databases used were APASS DR9 for the B and V ffilters (Henden *et al.* 2015),

Table 2. Filters used.

Filter	*LCO Description (Name)*	*Wavelength Center (Å)*	*Width (Å)*
B	Bessell B (blue)	4361	890
V	Bessell V (visual)	5448	840
ip	SDSS i' (i-prime)	7545	1290
zs	Pan-STARRS z_s (z-short)	8700	1040

Note: The values for wavelength center, and width, (angstroms) are tabulated on LCO's webpages and are derived from transmission data.

Table 3. Telescope locations and the number of observations taken.

Location	*LCO Label*	*Number of Observations*
SAAO, Sutherland, South Africa	kb87	30
CTIO, Region IV, Chile	kb29	21
Haleakala Observatory, Maui, USA	kb27	15
CTIO, Region IV, Chile	kb26	12
Tiede Observatory, Tenerife, Spain	kb95	11
Siding Spring Observatory, NSW, Australia	kb88	9
McDonald Observatory, Texas, USA	kb55	8
Tiede Observatory, Tenerife, Spain	kb82	8
Tiede Observatory, Tenerife, Spain	kb56	3
Siding Spring Observatory, NSW, Australia	kb24	2
Tiede Observatory, Tenerife, Spain	kb96	1

Note: SAAO, South African Astronomical Observatory; CTIO, Cerro Tololo Inter-American Observatory.

Skymapper DR 1.1 for the ip filter (Wolf *et al.* 2018), and Pan-STARRS for the zs filter (Magnier *et al.* 2020; Flewelling *et al.* 2020). Reduction to the magnitude system is performed and light curves are plotted for the observed variable star, WZ Hya, using differential photometry.

All calibration stars used are provided in Table 4 along with their R.A., Dec., and magnitude. Out of the six methods available, the SEK method provided the cleanest light curves and these magnitudes were used in this paper. Astrosource also creates a list of all magnitude measurements that were recovered in each method. The SEK method provided 103 in the B filter, 109 in the V filter, 46 in the ip filter, and 107 in the zs filter.

3. Results

In this section, we will discuss the derivation of the period, metallicity, absolute magnitude, and apparent magnitude of WZ Hya. We will then discuss the calculated distance using these quantities.

Table 4. List of comparison stars shown in Figure 1 with their calibrated magnitudes from the three surveys listed in the text.

Label	*Name*	*R.A. (°)*	*Dec. (°)*	*B Magnitude*	*V Magnitude*	*ip Magnitude*	*zs Magnitude*
CS1	TYC 5496–399–1	153.2930114	–13.2281205	—	11.392 ± .0197	11.024 ± .0156	—
CS2	TYC 5496–179–1	153.3767936	–13.2490501	—	11.329 ± .0223	11.053 ± .0168	—
CS3	UCAC4 384–056646	153.2681133	–13.3101129	—	12.321 ± .0303	11.673 ± .0177	—
CS4	TYC 5496–549–1	153.2548302	–13.0648543	—	11.601 ± .0275	11.409 ± .0183	11.272 ± .2996
CS5	UCAC4 385–056463	153.3065883	–13.1980118	—	12.947 ± .0397	12.289 ± .0247	11.998 ± .2302
CS6	UCAC4 385–056484	153.4398068	–13.1333245	—	12.250 ± .0441	11.692 ± .0152	11.434 ± .2887
CS7	TYC 5496–502–1	153.4004762	–13.2669225	—	11.360 ± .0415	10.998 ± .0163	—
CS8	UCAC4 384–056658	153.3415656	–13.2961601	—	12.887 ± .0498	12.096 ± .0229	11.766 ± .2536
CS9	UCAC4 386–056121	153.3904497	–12.9817688	—	12.841 ± .0526	12.436 ± .0291	12.237 ± .2129
CS10	TYC 5496–594–1	153.4185244	–13.1498112	12.782 ± .03	—	11.131 ± .0121	—
CS11	TYC 5496–141–1	153.4836995	–13.2713872	—	—	10.636 ± .0221	—
CS12	TYC 5496–559–1	153.2353099	–12.9970765	—	—	11.303 ± .0181	—

3.1. Period

Period finding and light curves were produced by AstroSource. Two different methods were used to obtain the period, string length minimization (String) (Dworetsky 1983) and phase dispersion minimization method (PDM) (Stellingwerf 1978). These are both standard methods and have the advantage of being model-independent. The only assumption made is the repeating signal, in this case, the period. Altunin *et al.* (2020) developed a method that automates these processes across data sets, this being the method used within AstroSource. Figure 2 presents all four light curves provided through the PDM. These light curves show the characteristic "shark tooth" shape of an RRab-type star.

We now take a look to see if our light curves are adequately sampled to produce a convincing distance measurement. The curves produced for the B, V, and zs bands all have over 100 magnitude inputs, while the ip band only has 46 inputs. The light curves from all four bands clearly showcase the rise and fall of the apparent magnitude with several points clustered around the extrema and therefore are considered sufficient for determining a period and an average magnitude.

The period of WZ Hya was determined by taking the weighted average of the eight values in Table 5. This results in the value of 0.5377 ± 0.0005 day. This value closely resembles those of other studies listed in Table 6.

3.2. Fourier decomposition

Fourier decomposition of the observed light curves of RR Lyr stars is an important analysis technique because physical parameters of these stars are shown to be correlated with the so-called relative Fourier parameters (e.g., Jurcsik and Kovacs (1996), Kovács (2005), Arellano Ferro (2022)). We fit a sine series of the form:

$$m(t) = A_0 + \sum_{j=1}^{N} A_j \sin(j\omega(t - t_0) + \varphi_j) \quad (2)$$

where m(t) is the model magnitude at time t, t_0 is the epoch of maximum light, A_j are the amplitudes to be fit, $\omega = 2\pi / P$ is the frequency of variation, P is the period of variation, φ_j are the phase shifts to be fit, and N is the order of the fit. The relative Fourier parameters are defined:

$$A_{ij} = \frac{A_i}{A_j}, \quad (3)$$

$$\varphi_{ij} = j\varphi_i - i\varphi_j. \quad (4)$$

The data were period folded using the modal period 0.537729 day. We used the Python3 package scipy.optimize.leastsq to minimize the residuals between the measured magnitudes and model magnitudes. The question of how many sines to fit is an open one; we decided upon N = 11 for B-, V-, and zs-band and N = 6 for ip-band for reasons discussed in the next two paragraphs.

As an upper limit to the order of the fit, N, we chose two times the ratio of the total number of data points to the number of data points in the peak. The rationale is derived from Nyquist-Shannon sampling theory. The light curve changes most rapidly near maximum light, i.e., the light curve is sharply peaked. It is crucial to estimate as precisely as possible the epoch of maximum light, t_0, because the values of the Fourier phase parameters depend sensitively upon the value of t_0. By Shannon's theorem, to sample adequately the shape of the light curve near the peak we need a high enough frequency so that two complete sine waves fit within the peak. How wide is the peak? To estimate the width we first estimated the amplitude of the light curve, then counted the number of data points whose values were brighter than the half-amplitude. The ratio of the number of data points in the peak to the total number of data points is thus an estimate of the full width at half maximum (FWHM) of the (phased) light curve. The inverse of this ratio is the number of times the light curve is wider than the FWHM. Twice this number is an upper limit to the order of the fit, N. In V-band there are 15 data points of 109 total representing the peak, so $N \approx 2 \times 109 / 15$ is approximately 14.

In practice, we found that N = 14 was an "over fit," i.e., the higher order sines try to fit the scatter. The reader's attention is directed to Figure 3, and note the light curve is poorly sampled near a phase of 0.1. At orders of N > 12 a prominent peak appears there; there are no data points to contribute to the value of χ^2 in the optimization process and thus constrain these higher orders of sine. The N = 11 fit in Figure 3 may also have the slightest of bumps at this location, but we ran into a different problem for fits of N < 11. For a lower order fit the

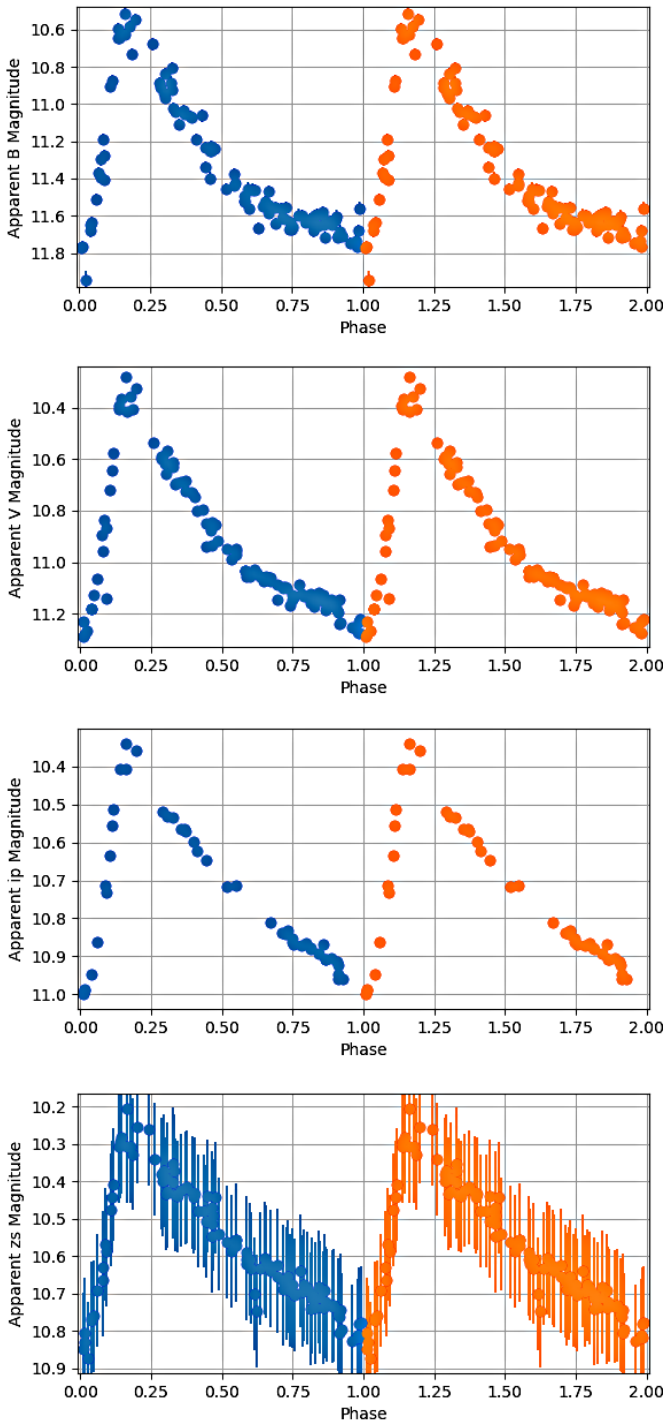

Figure 2. Light curves for WZ Hya in order from top to bottom: B, V, ip, and zs bands. All of these light curves are from the PDM method. Two full cycles are showcased to better visualize the shape of the curve. Calibrated magnitudes for each filter are shown in Table 7. Period values for each filter are provided in Table 5. No explicit choice was made for the value of phase.

Table 5. Period values in days determined through both PDM and String methods.

Filter	*PDM (days)*	*String (days)*
B	0.537635 ±.00114	0.537729 ±.001519
V	0.537920 ±.00114	0.537729 ±.001473
ip	0.537729 ±.001235	0.537729 ±.001758
zs	0.537729 ±.00114	0.537729 ±.001473

Note: PDM, phase dispersion minimization method; String, string length minimization method.

Table 6. List of known period values for WZ Hya from past studies.

Period (days)	*Source*
0.54	Joy (1950)
0.538	McNamara and Langford (1969)
0.53771535	Clube *et al.* (1969)
0.538	Jones (1973)
0.538	Hemenway (1975)
0.5377	Strauss (1976)
0.538	Preston *et al.* (1991)
0.5377229	Fernley *et al.* (1993)
0.538	Eggen (1994)
0.537718	Kovács (2005)
0.537713	Feast *et al.* (2008)
0.53772	Kolenberg and Bagnulo (2009)
0.5377	Dambis *et al.* (2013)
0.5373193	Skarka (2014)
0.537713	Gavrilchenko *et al.* (2014)
0.5377	Marsakov *et al.* (2018)

Table 7. Fourier decomposition parameters, and values derived therefrom, extracted from a least squares fit of a sine series to each light curve.

Filter	A_0 *(mag)*	*Amplitude (mag)*	σ_{31} *(rad*	*Epoch oft Maximum Light*
B	11.31 ± 0.09	0.73	—	—
V	10.91 ± 0.09	0.58	5.25	2459633.0312
ip	10.72 ± 0.15	0.37	—	—
zs	10.57 ± 0.14	0.29	—	—

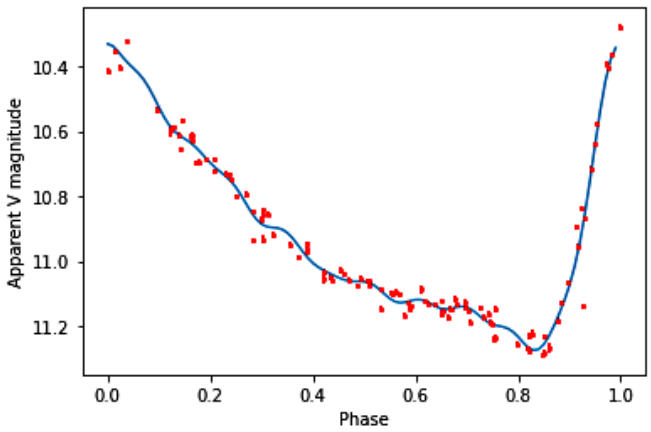

Figure 3. Phased light curve in V-band (points) with an 11th-order sine series fit (curve). Phase zero is at maximum light.

value of φ_1 experiences a large jump, and the inferred values of iron abundance are highly unrealistic. So we were left a single value, N = 11, that produced a reasonable fit for B, V, and zs light curves, an uncomfortably specific value, and perhaps an ungentle reminder that one can never have too much data. For the remaining filter, ip, there are about half as many total data points, and sine series at N > 6 showed noise-fitting. It is noted that the values of the intensity means, A_0, do not depend sensitively to the order of fit, and all values of A_0 were very close to the values of the various means discussed in section 3.4.

The relevant decomposition parameters for the purpose of this study are the zeroth order amplitudes, A_0, and the first and third order phases, φ_1 and φ_3. The zeroth order amplitude values for each filter are adopted as average apparent magnitudes, (m). The first and third order phases are extracted from the V-band data only and are used to compute iron abundance. The epoch of maximum light is a barycentric julian date (BJD) computed from the fit using the PYTHON3 package scipy.optimize.fmin. The results are tabulated in Table 7.

3.3. Metallicity

Iron abundances found in other projects are showcased in Table 8, where a total of eight different values were found. The [Fe/H] of –1.40 from Eggen (1994) was derived photometrically by comparison with model atmospheres from Lester *et al.* (1986) assuming log(g) = 2.75. The –1.39 value from Fernley *et al.* (1998) uses Hipparcos data. The values of −1.30 (Layden 1994) and −0.89 (Norris 1986) were both derived using spectroscopy. The Gaia Data Release 3 (DR3) derives a [Fe/H] of –0.8574 (Gaia Collaboration 2022). We discovered that the value of –1.04 from Kovács (2005) appeared to be incorrect, as it is different than the value found in the references of that paper. The value of –0.59 from Ammons *et al.* (2006) also raised concern since it was derived using a training set of FGK dwarf stars only, not evolved stars, using Tycho data. The –1.32 value from Anderson and Francis (2012) uniquely assigns homogenized abundances to Hipparcos stars from a literature survey.

We derived an iron abundance value from the Fourier parameters thus (Jurcsik and Kovacs 1996):

$$[Fe/H] = -5.038 - 5.394P + 1.345\varphi_{31}, \quad (5)$$

to obtain a value of [Fe/H] = –0.882. Our value is consistent with the larger of the historical values. The error on the φ_{31} term is large, of order 1 radian.

Using this iron abundance value, we can convert it into a metals/hydrogen ratio [M/H] via (Salaris *et al.* 1993):

$$[M/H] = [Fe/H] + \log(0.638 \times 10^{0.3} + 0.362). \quad (6)$$

This gives us a [M/H]} value of –0.668 which we can then apply to a conversion to log(Z) via (Catelan *et al.* 2004):

$$\log Z = [M/H] - 1.765. \quad (7)$$

This gives us a log Z value of –2.43.

Table 8. List of derived metallicity values from past studies.

[Fe/H]	*Reference*
–1.40	Eggen (1994)
–1.39	Fernley *et al.* (1998)
–1.32	Anderson and Francis (2012)
–1.30	Layden (1994)
–1.04	Kovács (2005) (spurious?)
–0.89	Norris (1986)
–0.8574	Gaia Collaboration (2022)
–0.59	Ammons *et al.* (2006)

3.4. Apparent and absolute magnitude

An incomplete reading of the literature reveals four methods by which an average apparent magnitude can be computed for a variable star. These four are the magnitude-weight mean, $(m)_{mag}$, the intensity-weighted mean, $(m)_{int}$, the phase-weighted mean, $(m)_{pha}$ (Saha and Hoessel 1990), and the mean derived from Fourier decomposition, which is called the intensity mean, $(m)_{fou}$. For n data points with ith magnitude m_i at relative phase Φ_i the definitions are listed:

$$(m)_{mag} = \frac{1}{n}\sum^{n} m_i \quad (8)$$

$$(m)_{int} = -2.5 \log \frac{1}{n}\sum^{n} 10^{-0.4m_i} \quad (9)$$

$$(m)_{pha} = -2.5 \log \frac{1}{2}\sum^{n} (\Phi_{i+1} - \Phi_{i-1}) 10^{-0.4m_i} \quad (10)$$

$$(m)_{fou} = A_0 \quad (11)$$

Note that the data must be phase-sorted before computing the phase-weighted mean.

Each mean has its own merits and the same goal, viz., to best approximate the flux of the "static" condition of the star. The values of the various means for our data are so close to each other as to be statistically indistinguishable. We adopt the Fourier decomposition amplitudes listed in Table 7 for the mean apparent magnitudes; to do so is consistent with modern practice and internally consistent with our computation of iron abundance.

Absolute magnitudes for WZ Hya were obtained using three magnitude-metallicity relations. The M_v-metallicity relation is from Catelan *et al.* (2004) while the M_i and M_z-metallicity relations are from Cáceres and Catelan (2008):

$$M_V = 2.288 + 0.882 \log Z + 0.108(\log Z)^2 \quad (12)$$

$$M_i = 0.908 - 1.035 \log P + 0.220 \log Z \quad (13)$$

$$M_z = 0.839 - 1.295 \log P + 0.211 \log Z \quad (14)$$

In these equations, M is the absolute magnitude of the source star, P is the period (days), and Z is the metallicity.

3.5. Distance

Using the distance modulus equation, we can solve for our distance and interstellar extinction simultaneously by plugging in our apparent and absolute magnitudes:

$$d = 10^{(m - M - A + 5)/5} \quad (15)$$

In this equation, m is the average apparent magnitude, M is the absolute magnitude, and A is the value for interstellar extinction. The color excess E(B–V) was found using the three distances and their associated extinction values derived in each of the V, ip, and zs filters: d_V, d_{ip}, d_{zs}; A_V, A_{ip}, A_{zs}. This was done using the standard relations for extinction, e.g.,

$$R_\upsilon = \frac{A\upsilon}{E(B–V)} \quad (16)$$

where $R_\upsilon = 3.1$. A color excess of E(B–V) = 0.142 mag was derived by minimizing the standard deviation of the V, ip, and zs distances. Changing the color excess resulted in the distances having larger differences between each filter. If our distances were measured perfectly, we would expect a color excess value that gives identical distances in each filter. However, this did not happen, and we believe our value is a global minimum of the standard deviation.

An estimate of the maximum extinction along the line of sight to WZ Hya is provided by Schlafly and Finkbeiner (2011) and Schlegel *et al.* (1998) via online query of the NASA/IPAC Infrared Science Archive. They provide two mean extinction values, 0.0700 ± 0.0011 (Schlafly and Finkbeiner 2011) and 0.0814 ± 0.0012 (Schlegel *et al.* 1998). The distances determined using each of the different color excess values are provided in Table 9.

The final distance value calculated was an error-weighted average of the three distances in each filter. This is represented in the last row of Table 9, where we produced an average distance of 872 ± 47 parsecs. Comparing this value to the Gaia DR3 value of 999 ± 16 parsecs (Gaia Collaboration 2022), the difference between the calculated value and the Gaia DR3 value is nearly 2 standard deviations. When using the Schlafly and Finkbeiner (2011) and Schlegel *et al.* (1998) color excess values, we get an average distance of 942 ± 51 and 931 ± 50 parsecs, respectively. These two values are within 1 standard deviation of the Gaia DR3 distance value.

Table 9. Distances in each filter.

		Distances (pc)	
E(B–V)	0.142	0.0700 ± 0.0011	0.0814 ± 0.0012
V	866 ± 73	960 ± 81	945 ± 80
ip	898 ± 94	964 ± 101	953 ± 100
zs	862 ± 82	907 ± 86	900 ± 85

Note: Distances in each filter with its corresponding E(B–V) measurement; (d) represents the weighted average distance of the V, ip, and zs filters.

4. Conclusion

Using observations of the RR Lyr star WZ Hya, this research tested the infrared period-luminosity-metallicity (PLZ) relationships of Catelan *et al.* (2004) and Cáceres and Catelan (2008). The period was determined to be 0.5377 ± 0.0005 day. The photometric distance to WZ Hya was determined to be 872 ± 47 parsecs, 942 ± 51, and 931 ± 50 parsecs using the color excess derived using our minimization method, and the provided values from Schlafly and Finkbeiner (2011) and Schlegel *et al.* (1998) respectively. These values agreed with the Gaia DR3 value of 999 ± 16 within 1–2 standard deviations. The infrared PLZ relations yielded distances consistent with the Gaia parallax distance. For this particular star, the ip filter distance was closest to the Gaia distance; it will be interesting to see if this closest agreement is generally true.

5. Acknowledgements

Thank you to Michael Fitzgerald for creating the OurSolarSiblings RR Lyrae research course, providing access to an efficient pipeline, providing educational materials, and also providing telescope time with the Las Cumbres Observatory.

Many thanks to the editor and anonymous referee for the careful review and meaningful comments that improved the manuscript.

The DSS image is based on photographic data obtained using The UK Schmidt Telescope. The UK Schmidt Telescope was operated by the Royal Observatory Edinburgh, with funding from the UK Science and Engineering Research Council, until 1988 June, and thereafter by the Anglo-Australian Observatory. Original plate material is copyright (c) the Royal Observatory Edinburgh and the Anglo-Australian Observatory. The plates were processed into the present compressed digital form with their permission. The Digitized Sky Survey was produced at the Space Telescope Science Institute under US Government grant NAG W-2166.

This research has made use of SAOImageDS9, developed by Smithsonian Astrophysical Observatory.

This work has made use of data from the European Space Agency (ESA) mission Gaia (https://www.cosmos.esa.int/Gaia), processed by the Gaia Data Processing and Analysis Consortium (DPAC, https://www.cosmos.esa.int/web/Gaia/dpac/consortium). Funding for the DPAC has been provided by national institutions, in particular, the institutions participating in the Gaia Multilateral Agreement.

This research has made use of the NASA/IPAC Infrared Science Archive, which is funded by the National Aeronautics and Space Administration and operated by the California Institute of Technology.

This research has made use of the SIMBAD database, operated at CDS, Strasbourg, France.

This research has made use of the APASS database, located at the AAVSO web site. Funding for APASS has been provided by the Robert Martin Ayers Sciences Fund.

References

Alonso-García, J., Mateo, M., Sen, B., Banerjee, M., Catelan, M., Minniti, D., and von Braun, K. 2012, *Astron. J.*, **143**, 70 (DOI: 10.1088/0004-6256/143/3/70).

Altunin, I., Caputo, R., and Tock, K. 2020, *Astron. Theory Obs. Methods*, **1**, 1 (DOI: 10.32374/atom.2020.1.1).

Ammons, S. M., Robinson, S. E., Strader, J., Laughlin, G., Fischer, D., and Wolf, A. 2006, *Astrophys. J.*, **638**, 1004 (DOI: 10.1086/498490).

Anderson, E., and Francis, C. 2012, *Astron. Lett.*, **38**, 331 (DOI: 10.1134/S1063773712050015).

Arellano Ferro, A. 2022, *Rev. Mex. Astron. Astrofis.*, **58**, 257 (DOI: 10.22201/ia.01851101p.2022.58.02.08).

Barbier-Brossat, M., Petit, M., and Figon, P. 1994, *Astron. Astrophys., Suppl. Ser.*, **108**, 603.

Bertin, E. 2011, in *Astronomical Data Analysis Software and Systems XX*, eds. I. N. Evans, A. Accomazzi, D. J. Mink, A. H. Rots, ASP Conf. Proc. 442, Astronomical Society of the Pacific, San Francisco, 435.

Bertin, E., and Arnouts, S. 1996, *Astron. Astrophys., Suppl. Ser.*, 117, 393 (DOI: 10.1051/aas:1996164).

Bessell, M. S. 1993, in *Stellar Photometry—Current Techniques and Future Developments*, eds. C. J. Butler, I. Elliott, IAU Colloq. 136, Cambridge Univ. Press, Cambridge, 22.

Brown, T. M., *et al.* 2013, *Publ. Astron. Soc. Pacific,* **125**, 1031 (DOI: 10.1086/673168).

Cáceres, C., and Catelan, M. 2008, *Astrophys. J., Suppl. Ser.*, **179**, 242 (DOI: 10.1086/591231).

Catelan, M., Pritzl, B. J., and Smith, H. A. 2004, *Astrophys. J., Suppl. Ser.*, **154**, 633 (DOI: 10.1086/422916).

Clube, S. V. M., Evans, D. S., and Jones, D. H. P. 1969, *Mem. Roy. Astron. Soc.*, **72**, 101.

Collins, K. A., Kielkopf, J. F., Stassun, K. G., and Hessman, F. V. 2017, *Astron. J.*, **153**, 77 (DOI: 10.3847/1538-3881/153/2/77).

Dambis, A. K., Berdnikov, L. N., Kniazev, A. Y., Kravtsov, V. V., Rastorguev, A. S., Sefako, R., and Vozyakova, O. V. 2013, *Mon. Not. Roy. Astron. Soc.*, **435**, 3206 (DOI: 10.1093/mnras/stt1514).

Dworetsky, M. M. 1983, *Mon. Not. Roy. Astron. Soc.*, **203**, 917 (DOI: 10.1093/mnras/203.4.917).

Eggen, O. J. 1994, *Astron. J.*, **107**, 2131 (DOI: 10.1086/117024).

Feast, M. W., Laney, C. D., Kinman, T. D., van Leeuwen, F., and Whitelock, P. A. 2008, *Mon. Not. Roy. Astron. Soc.*, **386**, 2115 (DOI: 10.1111/j.1365-2966.2008.13181.x).

Fernley, J. A., Skillen, I., and Burki, G. 1993, *Astron. Astrophys., Suppl. Ser.*, **97**, 815

Fernley, J., Barnes, T. G., Skillen, I., Hawley, S. L., Hanley, C. J., Evans, D. W., Solano, E., and Garrido, R. 1998, *Astron. Astrophys.*, **330**, 515.

Fitzgerald, M. T. 2018, *Robotic Telesc. Student Res. Educ. Proc.*, **1**, 347.

Fitzgerald, M., Gomez, E., Salimpour, S., and Wibowo, R. 2020, *J. Open Source Software*, in review.

Flewelling, H. A., *et al.* 2020, *Astrophys. J., Suppl. Ser.*, **251**, 7 (DOI: 10.3847/1538-4365/abb82d).

Fukugita, M., Ichikawa, T., Gunn, J. E., Doi, M., Shimasaku, K., and Schneider, D. P. 1996, *Astron. J.*, **111**, 1748 (DOI: 10.1086/117915

Gaia Collaboration. 2022, VizieR Online Data Catalog, I/355.

Gavrilchenko, T., Klein, C. R., Bloom, J. S., and Richards, J. W. 2014, *Mon. Not. Roy. Astron. Soc.*, **441**, 715 (DOI: 10.1093/mnras/stu606).

Hemenway, M. K. 1975, *Astron. J.*, **80**, 199 (DOI: 10.1086/111732).

Henden, A. A., Levine, S., Terrell, D., and Welch, D. L. 2015, Amer. Astron. Soc. Meeting Abstr. 225, id.336.16.

Jones, D. H. P. 1973, *Astrophys. J., Suppl. Ser.*, **25**, 487 (DOI: 10.1086/190276).

Joy, A. H. 1950, *Publ. Astron. Soc. Pacific*, **62**, 60 (DOI: 10.1086/126230).

Jurcsik, J., and Kovacs, G. 1996, *Astron. Astrophys.*, **312**, 111.

Kolenberg, K., and Bagnulo, S. 2009, *Astron. Astrophys.*, **498**, 543 (DOI: 10.1051/0004-6361/200811591).

Kovács, G. 2005, *Astron. Astrophys.*, **438**, 227 (DOI: 10.1051/0004-6361:20052742).

Laher, R. R., Gorjian, V., Rebull, L. M., Masci, F. J., Fowler, J. W., Helou, G., Kulkarni, S. R., and Law, N. M. 2012a, *Publ. Astron. Soc. Pacific*, **124**, 737 (DOI: 10.1086/666883).

Laher, R. R., *et al.* 2012b, *Publ. Astron. Soc. Pacific*, **124**, 764 (DOI: 10.1086/666507).

Layden, A. C. 1994, *Astron. J.*, 108, 1016 (DOI: 10.1086/117132).

Lester, J. B., Gray, R. O., and Kurucz, R. L. 1986, *Astrophys. J., Suppl. Ser.*, **61**, 509 (DOI: 10.1086/191122

Magnier, E. A., *et al.* 2020, *Astrophys. J., Suppl. Ser.*, **251**, 3 (DOI: 10.3847/1538-4365/abb829).

Marsakov, V. A., Gozha, M. L., and Koval, V. V. 2018, *Astron. Rep.*, **62**, 50 (DOI: 10.1134/S1063772918010055).

McNamara, D. H., and Langford, W. R. 1969, *Publ. Astron. Soc. Pacific*, **81**, 141 (DOI: 10.1086/128753).

Norris, J. 1986, *Astrophys. J., Suppl. Ser.*, **61**, 667 (DOI: 10.1086/191128).

Preston, G. W., Shectman, S. A., and Beers, T. C. 1991, *Astrophys. J.*, **375**, 121 (DOI: 10.1086/170175).

Saha, A., and Hoessel, J. G. 1990, *Astron. J.*, **99**, 97 (DOI: 10.1086/115316).

Salaris, M., Chieffi, A., and Straniero, O. 1993, *Astrophys. J.*, **414**, 580 (DOI: 10.1086/173105).

Schechter, P. L., Mateo, M., and Saha, A. 1993, *Publ. Astron. Soc. Pacific*, **105**, 1342 (DOI: 10.1086/133316).

Schlafly, E. F., and Finkbeiner, D. P. 2011, *Astrophys. J.*, **737**, 103 (DOI: 10.1088/0004-637X/737/2/103).

Schlegel, D. J., Finkbeiner, D. P., and Davis, M. 1998, *Astrophys. J.*, **500**, 525 (DOI: 10.1086/305772).

Skarka, M. 2014, *Astron. Astrophys.*, **562A**, 90 (DOI: 10.1051/0004-6361/201322491).

Stellingwerf, R. F. 1978, *Astrophys. J.*, **224**, 953 (DOI: 10.1086/156444).

Stetson, P. B. 1987, *Publ. Astron. Soc. Pacific*, **99**, 191 (DOI: 10.1086/131977).

Strauss, F. M. 1976, *Publ. Astron. Soc. Pacific*, **88**, 531 (DOI: 10.1086/129980).

Tonry, J. L., *et al.* 2012, *Astrophys. J.*, **750**, 99 (DOI: 10.1088/0004-637X/750/2/99).

Wolf, C., *et al.* 2018, *Publ. Astron. Soc. Australia*, **35**, 10 (DOI: 10.1017/pasa.2018.5).

Appendix A. Data tables and source file locations.

Table A1. WZ Hya dataset.

JD	*Magnitude*	*Mag. Error*	*Filter*	*JD*	*Magnitude*	*Mag. Error*	*Filter*
2459631.32120815	11.68119776	0.03160651	B	2459711.62814068	10.92119465	0.03394172	B
2459631.38961681	10.90275832	0.03106498	B	2459711.81080307	11.47038469	0.03150432	B
2459631.52986586	11.05240500	0.03095381	B	2459715.53026930	11.52628126	0.03422700	B
2459631.90497966	11.36690333	0.03074839	B	2459715.53712212	11.45275452	0.03410839	B
2459632.11644435	11.25047690	0.03195777	B	2459715.74394376	11.76338112	0.03094872	B
2459632.31963406	11.59148747	0.03277155	B	2459715.92834665	10.88393288	0.03230447	B
2459632.46740585	10.87088978	0.03082018	B	2459716.19871550	11.62341197	0.03135328	B
2459632.65489512	11.39846061	0.03328912	B	2459716.31213507	11.64535232	0.03152462	B
2459632.84242209	11.63499130	0.03394055	B	2459716.47460922	11.04307744	0.03138095	B
2459633.02999621	10.51738172	0.03106159	B	2459716.74423077	11.65556754	0.03088464	B
2459633.33575260	11.55400480	0.03135752	B	2459716.84953994	11.68174912	0.03136323	B
2459633.40504647	11.57827082	0.03111393	B	2459717.37319755	11.76559009	0.03108308	B
2459633.96745447	11.62460656	0.03074584	B	2459717.50605679	10.67653244	0.03390063	B
2459634.71738339	10.94227464	0.03378873	B	2459717.59952549	11.06166094	0.03405958	B
2459634.90502241	11.54681989	0.03065391	B	2459717.97848694	10.64632403	0.03091745	B
2459635.35021620	11.24058850	0.03146099	B	2459718.36908144	11.64866183	0.03102339	B
2459635.46743325	11.55229917	0.03118107	B	2459719.36952073	11.61669957	0.03096378	B
2459641.59250689	11.18647574	0.03092746	B	2459719.47441348	11.68228870	0.03396045	B
2459656.50994394	11.68038804	0.03250783	B	2459720.37812455	11.55916872	0.03088135	B
2459656.52677103	11.60091458	0.03231762	B	2459720.58767248	11.56005704	0.03495183	B
2459656.70236651	10.73154939	0.03195103	B	2459720.61774372	11.63637107	0.03140771	B
2459657.63984314	11.70944913	0.03149046	B	2459721.20377867	10.59464812	0.03131397	B
2459697.85450335	11.56288489	0.03094733	B	2459721.38079223	11.22624726	0.03119094	B
2459698.22203357	11.06950416	0.03115582	B	2459721.54737673	11.59723452	0.03489259	B
2459698.36058325	11.52359494	0.03235234	B	2459721.74559132	10.64155750	0.03071132	B
2459698.49942127	11.71505990	0.03170587	B	2459724.45211563	10.58558601	0.03168327	B
2459698.74480662	11.03472327	0.03075865	B	2459724.53644186	11.02336458	0.03168203	B
2459699.46883935	11.61231692	0.03163601	B	2459725.37183316	11.63212235	0.03125886	B
2459699.81178139	11.10996455	0.03109777	B	2459725.47378102	11.29732681	0.03181294	B
2459700.20797593	11.27416993	0.03099031	B	2459725.74664321	11.49065338	0.03098182	B
2459700.56170047	11.67326501	0.03150321	B	2459725.86201528	11.63246256	0.03066522	B
2459700.93669469	11.23216378	0.03113684	B	2459726.37222211	11.63436081	0.03110716	B
2459701.60866620	11.64385517	0.03162460	B	2459726.45907937	11.60178023	0.03362850	B
2459701.87893299	10.54808932	0.03060532	B	2459726.74690490	11.34005042	0.03096944	B
2459702.21107926	11.61488492	0.03119212	B	2459726.78617987	11.45542248	0.03084804	B
2459702.25307245	11.64699553	0.03117435	B	2459727.45127671	11.65897289	0.03149027	B
2459702.46445447	10.90937105	0.03142435	B	2459727.53614328	11.70864622	0.03141469	B
2459702.62407697	11.51861527	0.03166141	B	2459727.74739230	10.96655069	0.03090420	B
2459703.01222885	10.83516455	0.03122663	B				
2459703.20806666	11.54491682	0.03123967	B	2459631.32176487	11.23098219	0.00856189	V
2459703.37407174	11.73321993	0.03115290	B	2459631.39015043	10.64091303	0.00721569	V
2459703.56145459	10.80511083	0.03329113	B	2459631.53039949	10.72417289	0.00705874	V
2459704.21840146	11.37270534	0.03120304	B	2459632.11707044	10.87453853	0.01134212	V
2459704.34700364	11.60036503	0.03132903	B	2459632.32019080	11.11731306	0.00947455	V
2459704.50308852	11.39383704	0.03135875	B	2459632.46795089	10.57592942	0.00697907	V
2459704.82186830	11.58426964	0.03069995	B	2459632.65550975	10.93288188	0.01159176	V
2459705.20986664	11.06397141	0.03115627	B	2459632.84303669	11.16142437	0.01231007	V
2459705.24886522	11.25349236	0.03123569	B	2459633.03059999	10.27867799	0.00725113	V
2459705.43638178	11.63532744	0.03129773	B	2459633.33629775	11.10243631	0.00779396	V
2459705.62388413	10.62814720	0.03115146	B	2459633.40560320	11.12640516	0.00741145	V
2459705.83168486	11.43619693	0.03133891	B	2459633.96810466	11.16223956	0.00687267	V
2459706.41467827	11.66344575	0.03119400	B	2459634.71798657	10.61395811	0.01135391	V
2459706.61694132	11.77148836	0.03128924	B	2459634.90563778	11.07445225	0.00658723	V
2459707.37145955	11.18941986	0.03077553	B	2459635.35076154	10.85560333	0.00881935	V
2459707.61626139	11.71485261	0.03163603	B	2459635.46797837	11.08585632	0.00757545	V
2459707.84062034	10.88803630	0.03227036	B	2459641.59313320	10.83542052	0.00705794	V
2459708.20300464	11.74466829	0.03152550	B	2459656.51104560	11.17194067	0.00963212	V
2459708.25705697	11.51115410	0.03128736	B	2459656.52783905	11.14428889	0.00961167	V
2459708.52079102	11.42444598	0.03377139	B	2459656.70343464	10.40350315	0.00846187	V
2459708.62361516	11.67121932	0.03151273	B	2459656.89097394	10.98879612	0.00809554	V
2459708.81101966	11.40590600	0.03132924	B	2459657.40287331	10.91717737	0.00997281	V
2459709.21062183	11.60003075	0.03126306	B	2459657.83656025	10.58720370	0.00660642	V
2459711.24406055	11.45964726	0.03212920	B	2459697.85557120	11.09714568	0.00732102	V
2459711.24827957	11.46173082	0.03236761	B	2459698.22297260	10.73442405	0.00745519	V
2459711.46436722	11.94210063	0.04966275	B	2459698.36168461	11.05422447	0.00918399	V

Table continued on following pages

Table A1. WZ Hya dataset (cont.).

JD	Magnitude	Mag. Error	Filter
2459698.50049568	11.23969433	0.00861602	V
2459698.74586166	10.68447405	0.00651769	V
2459699.03989695	11.14771217	0.00980217	V
2459699.46993081	11.10195134	0.00847730	V
2459699.62965451	11.28136037	0.00778777	V
2459699.81285153	10.68612531	0.00704274	V
2459700.20891495	10.86889823	0.00726682	V
2459700.37622688	10.74723363	0.00694093	V
2459700.56277911	11.14551619	0.00837344	V
2459700.75464628	10.71708236	0.00883561	V
2459700.93783197	10.93734896	0.00887568	V
2459701.60962844	11.14611813	0.00839703	V
2459701.88005757	10.32340126	0.00646920	V
2459702.21201839	11.15215185	0.00765449	V
2459702.25402307	11.17305268	0.00766597	V
2459702.46556749	10.58925391	0.00848174	V
2459702.62514488	11.03482661	0.00925387	V
2459703.01338619	10.56776608	0.00727696	V
2459703.20901927	11.06038718	0.00766719	V
2459703.37501246	11.26942934	0.00771130	V
2459703.56240552	10.61354901	0.00961088	V
2459704.21934061	10.94614202	0.00768201	V
2459704.34794264	11.13112543	0.00783055	V
2459704.50418071	10.95543237	0.00825845	V
2459704.82294081	11.07248647	0.00710963	V
2459705.21081736	10.73000468	0.00781084	V
2459705.24981604	10.84387429	0.00757284	V
2459705.43747441	11.12169165	0.00766847	V
2459705.62483649	10.41454991	0.00729793	V
2459705.83275267	10.95852716	0.01709137	V
2459706.41577953	11.05726672	0.00819051	V
2459706.61791683	11.28995689	0.00787362	V
2459707.37259575	10.79954125	0.00702156	V
2459707.61722841	11.18693566	0.00846792	V
2459707.84168745	10.59820882	0.01846062	V
2459708.20395538	11.25515601	0.00826521	V
2459708.25799751	11.06648392	0.00786685	V
2459708.52174222	10.96959337	0.01075267	V
2459708.62457532	11.16709057	0.00814072	V
2459708.81208735	11.13919074	0.00878394	V
2459709.21158414	11.14890554	0.00771536	V
2459711.24501128	11.02939528	0.00921082	V
2459711.24921901	11.04083864	0.00950904	V
2459711.46546865	11.26678241	0.01718254	V
2459711.62909139	10.62733931	0.01019201	V
2459711.81186939	11.06169097	0.00818734	V
2459715.53080266	11.05629794	0.01122435	V
2459715.53766717	11.05015691	0.01140439	V
2459715.74461708	11.27660642	0.00738109	V
2459715.92895613	10.61621181	0.00873878	V
2459716.19926060	11.14692108	0.00792803	V
2459716.31268001	11.18195780	0.00811704	V
2459716.47522228	10.69353089	0.00811796	V
2459716.74484604	11.13306399	0.00713996	V
2459716.85017754	11.18345808	0.00770394	V
2459717.37382369	11.23152486	0.00742539	V
2459717.50660182	10.53477125	0.01066790	V
2459717.60007119	10.79610816	0.01092264	V
2459717.78764107	11.12338903	0.00692882	V
2459717.97910147	10.40680258	0.00730584	V
2459718.36970757	11.15434943	0.00725604	V
2459719.37013531	11.09513374	0.00721605	V
2459719.47494693	11.23484994	0.01076551	V
2459720.37878542	11.05745628	0.00728260	V
2459720.58820739	11.22309786	0.01167114	V
2459720.61831196	11.12943392	0.00791142	V
2459721.20432199	10.39271632	0.00773426	V
2459721.38140667	10.85896708	0.00754318	V
2459721.54791105	11.08756349	0.01157736	V
2459721.74619431	10.36299144	0.00659583	V
2459724.45271880	10.35538364	0.00837314	V
2459724.53705630	10.69822101	0.00860641	V
2459725.37245917	11.14425542	0.00761149	V
2459725.47439555	10.89453777	0.00890517	V
2459725.74724677	11.03215008	0.00731312	V
2459725.86262988	11.13448704	0.00667883	V
2459726.37284834	11.12660374	0.00731357	V
2459726.45961276	11.18783561	0.01025520	V
2459726.74750857	10.84896351	0.00721619	V
2459726.78679440	10.94964284	0.00706361	V
2459727.45191450	11.13825566	0.00834278	V
2459727.53675778	11.19343732	0.00829792	V
2459727.74800753	10.65509449	0.00711970	V
2459631.39053289	10.55648431	0.00550258	i
2459631.53077037	10.57147150	0.00529747	i
2459632.46832180	10.51417880	0.00536922	i
2459633.03102939	10.34082725	0.00504870	i
2459633.33666873	10.83253219	0.00592412	i
2459633.40597407	10.86805539	0.00567568	i
2459633.96853404	10.91254450	0.00486197	i
2459641.59358528	10.71475958	0.00541331	i
2459657.64048168	10.95837165	0.00639423	i
2459657.83613127	10.52081704	0.00458260	i
2459697.85515348	10.83825174	0.00550703	i
2459698.50005996	10.95926836	0.00648658	i
2459698.74543282	10.56608435	0.00450234	i
2459699.62927147	10.98523929	0.00546827	i
2459699.81241842	10.56391484	0.00555219	i
2459700.20854407	10.73064096	0.00591570	i
2459700.37578641	10.59950236	0.00516710	i
2459700.56233857	10.86244673	0.00621707	i
2459700.75421840	10.63401254	0.00693163	i
2459701.87961705	10.35774183	0.00460786	i
2459702.21164739	10.88185558	0.00592165	i
2459703.56203461	10.53556247	0.00662110	i
2459704.21896959	10.71268025	0.00576139	i
2459704.82249749	10.81136101	0.00540506	i
2459705.43703406	10.87886264	0.00572599	i
2459705.62446111	10.40582789	0.00508036	i
2459706.61752665	10.99825287	0.00561892	i
2459707.37212047	10.62262219	0.00530269	i
2459707.61685294	10.90823369	0.00598006	i
2459708.25763665	10.86089016	0.00612845	i
2459716.74526366	10.89395946	0.00533096	i
2459716.85061799	10.94597944	0.00577784	i
2459717.37426410	10.98983883	0.00570631	i
2459717.78807034	10.87161034	0.00526509	i
2459717.97953064	10.40772908	0.00512816	i
2459718.37014800	10.90677193	0.00541374	i
2459719.37058731	10.83969881	0.00545159	i
2459725.37289954	10.90442091	0.00556959	i
2459725.86305866	10.86428269	0.00493983	i
2459726.37328883	10.85175947	0.00544215	i
2459726.45999521	10.92425839	0.00736830	i
2459726.74793789	10.64778762	0.00534345	i
2459726.78722322	10.71529874	0.00508839	i
2459727.45234329	10.86710720	0.00684808	i
2459727.53718664	10.94756530	0.00643976	i
2459727.74844838	10.53023937	0.00543720	i

Table continued on next page

Table A1. WZ Hya dataset (cont.).

JD	*Magnitude*	*Mag. Error*	*Filter*	*JD*	*Magnitude*	*Mag. Error*	*Filter*
2459631.32285389	10.78203507	0.15050933	z	2459705.62556718	10.30622256	0.15035184	z
2459631.39125106	10.44145689	0.15037791	z	2459705.83352896	10.57153671	0.15175672	z
2459631.53148860	10.41457243	0.15036347	z	2459706.41656708	10.63273065	0.15039274	z
2459632.11829888	10.51429645	0.15107269	z	2459706.61864831	10.84991407	0.15036729	z
2459632.32127990	10.68290595	0.15045219	z	2459707.37338343	10.47932695	0.15036470	z
2459632.46905161	10.40879291	0.15037393	z	2459707.61795928	10.73177187	0.15038634	z
2459632.65671485	10.54846137	0.15069227	z	2459707.84248661	10.37995546	0.15039250	z
2459632.84425321	10.74078865	0.15071855	z	2459708.20468500	10.82645355	0.15044368	z
2459633.03180580	10.20578020	0.15035893	z	2459708.25873876	10.69276995	0.15041935	z
2459633.33738765	10.65440540	0.15040000	z	2459708.52247260	10.55779694	0.15048733	z
2459633.40669219	10.69151655	0.15038322	z	2459708.62530269	10.69138020	0.15038106	z
2459633.61219789	10.26104776	0.15079467	z	2459711.24574090	10.70157326	0.15054014	z
2459634.71919207	10.43255192	0.15059871	z	2459711.24994864	10.74628830	0.15056297	z
2459634.90687842	10.60521655	0.15032782	z	2459711.46625629	10.87348393	0.15095943	z
2459635.35185058	10.44398231	0.15045952	z	2459711.62980942	10.37257327	0.15044954	z
2459635.46906738	10.62479420	0.15040014	z	2459711.81265709	10.63315095	0.15041091	z
2459641.59438461	10.56951199	0.15034931	z	2459715.53189182	10.62255017	0.15049505	z
2459656.51183339	10.73745108	0.15048501	z	2459715.53875619	10.60998373	0.15049361	z
2459656.52865002	10.73805249	0.15049498	z	2459715.74582272	10.81938025	0.15035631	z
2459656.70421063	10.32752091	0.15043448	z	2459715.93015837	10.35294804	0.15044921	z
2459656.89175564	10.58843782	0.15048595	z	2459716.20034952	10.71395361	0.15042301	z
2459657.40367260	10.54138680	0.15061632	z	2459716.31378054	10.76464077	0.15041905	z
2459657.83733875	10.37171322	0.15032388	z	2459716.47647730	10.44080625	0.15039559	z
2459697.85635923	10.66794176	0.15036657	z	2459716.74604015	10.70996851	0.15035387	z
2459698.22369076	10.44339064	0.15038915	z	2459716.85139407	10.77317511	0.15035629	z
2459698.36248389	10.61391133	0.15046186	z	2459717.37505188	10.80698922	0.15037017	z
2459698.50127352	10.80727223	0.15042284	z	2459717.50770247	10.34136831	0.15046219	z
2459698.74664934	10.41908558	0.15031886	z	2459717.60116024	10.47915679	0.15044534	z
2459699.04074243	10.74314577	0.15058538	z	2459717.78884682	10.69365887	0.15035474	z
2459699.47071848	10.68866258	0.15042033	z	2459717.98034193	10.29610808	0.15034050	z
2459699.63037953	10.82987728	0.15036386	z	2459718.37093561	10.72408285	0.15034985	z
2459699.81363279	10.42392521	0.15035116	z	2459719.37137499	10.67300351	0.15036255	z
2459700.20964455	10.58593233	0.15040116	z	2459719.47605906	10.79635613	0.15046105	z
2459700.37702606	10.43449585	0.15034688	z	2459720.38002633	10.63225237	0.15034784	z
2459700.56355515	10.69399312	0.15040903	z	2459720.58929645	10.77713829	0.15050392	z
2459700.75543019	10.47759611	0.15047198	z	2459720.61943562	10.76084938	0.15037456	z
2459700.93864325	10.43936531	0.15036992	z	2459721.20541182	10.30646149	0.15039970	z
2459701.61035802	10.65538088	0.15041941	z	2459721.38265799	10.49055559	0.15035776	z
2459701.88085672	10.25586391	0.15032545	z	2459721.54900010	10.63911151	0.15046978	z
2459702.21274797	10.71225491	0.15039709	z	2459721.74741067	10.28383230	0.15033698	z
2459702.25475276	10.73110322	0.15039950	z	2459724.45392371	10.30699905	0.15045869	z
2459702.46635516	10.39809275	0.15048897	z	2459724.53827339	10.43729983	0.15043322	z
2459702.62593252	10.60782518	0.15048067	z	2459725.37368720	10.73404219	0.15036833	z
2459703.01419464	10.42832482	0.15036998	z	2459725.47560047	10.63040382	0.15041861	z
2459703.20974908	10.62612274	0.15040716	z	2459725.74846399	10.59045759	0.15035685	z
2459703.37574511	10.81123895	0.15039881	z	2459725.86383466	10.68653769	0.15032462	z
2459703.56313515	10.40234977	0.15041641	z	2459726.37407647	10.67511115	0.15035774	z
2459704.22007019	10.55545715	0.15038940	z	2459726.46071340	10.75733677	0.15046591	z
2459704.34867282	10.67777937	0.15040493	z	2459726.74871439	10.50824590	0.15036044	z
2459704.50496849	10.66550237	0.15039720	z	2459726.78799930	10.56199176	0.15034503	z
2459704.82371899	10.63877824	0.15036971	z	2459727.45313099	10.70535056	0.15045880	z
2459705.21154701	10.43029152	0.15041051	z	2459727.53795122	10.76124796	0.15041864	z
2459705.25054560	10.47100007	0.15040380	z	2459727.74922477	10.39382015	0.15037274	z
2459705.43827371	10.70135120	0.15039738	z				

Table A2. Repository of the data files.

Available through the AAVSO ftp public datasets site
ftp://ftp.aavso.org/public/datasets/3850-Ritterby-511-wzhya/B-filter.txt
ftp://ftp.aavso.org/public/datasets/3850-Ritterby-511-wzhya/V-filter.txt
ftp://ftp.aavso.org/public/datasets/3850-Ritterby-511-wzhya/i-filter.txt
ftp://ftp.aavso.org/public/datasets/3850-Ritterby-511-wzhya/z-filter.txt